Ecological Questions 36 (2025) 4: 45–64 http://dx.doi.org/10.12775/EQ.2025.034

Identification of human interference and its impact on forest canopy density in the forested areas of Odisha, India

Tanushree Basu Roy, Dipanwita Dutta*

Department of Remote Sensing and GIS, Vidyasagar University, Midnapore, West Bengal, India
* Corresponding author: duttarsgisvu@gmail.com

Received: 5 May 2025 / Accepted: 26 September 2025

Abstract. Forests are among the most vital and indispensable components of our ecosystems. However, increasing population pressure and associated infrastructural development have led to significant degradation of forest resources, particularly in developing regions. This study examines the temporal dynamics of forest canopy density over a 30-year period and identifies areas of disturbance within the forested landscapes of Keonjhar and Sundargarh districts, situated in northern and north-western Odisha, India. Forest canopy density changes were assessed using Landsat imagery from 1988 and 2021. Remote sensing-based biophysical indices such as AVI, BSI, and SSI were employed to develop a forest canopy density (FCD) model. Results indicate that approximately 17% of the forested area has been converted to bare land, and nearly 10% of the dense and moderately dense forested area has been converted to open forest in this period. Additionally, secondary datasets, including road networks, railway lines, mining areas, settlements, and industrial zones were integrated to analyze human-induced disturbances and delineate disturbance zones within the forests. A trend analysis of NDVI from 1988 to 2021 was conducted to validate these zones. Increasing mining activities, infrastructure development, settlement growth, and industrial waste dumping are identified as primary contributors to the increasing disturbance within the forest ecosystems of Keonjhar and Sundargarh districts. These findings highlight the urgent need for sustainable forest management and conservation strategies in this region.

Keywords: deforestation, mining, anthropogenic disturbance, FCD, NDVI, trend analysis.

1. Introduction

Forests play a critical role in regulating both biotic and abiotic components of the Earth's environment (Hernández-Clemente et al., 2019; Radhakrishnan et al., 2020). They influence ecosystem dynamics and serve as vital resources, supporting land stability, water cycles, and providing habitats for a vast array of species (Mengist et al., 2021; Sahana et al., 2015). Therefore, protecting and assessing forest health has become a major concern for sustainable resource management (Estoque et al., 2021; O'Laughlin et al., 1994; Pei et al., 2021). Forest degradation is a widespread issue with significant impacts on the environment and biodiversity (Bragagnolo et al., 2021; Grecchi et al., 2017; Sharma et al., 2020; Vancutsem et al., 2021). According to the Food and Agriculture Organization of the United Nations (FAO, 2010), the average annual global forest cover loss over the past decade has been approximately 5.2 million hectares. This trend of significant forest loss is particularly evident in the Keonjhar and Sundargarh districts of Odisha, India, which have faced major ecological changes in recent decades. The rapid expansion of mining and industrial zones has led to extensive forest areas being converted into collieries, settlements, and fallow lands. This

prolonged, large-scale mining practice fundamentally alters the landscape's structure, diminishes its ecological capacity, depletes land resources, and gives rise to numerous critical environmental challenges. As a consequence of mining-related dust and other problems, chlorophyll absorption and cellular vigor are being reduced, which adversely affects the health of surrounding vegetation (Gupta et al., 2024). Therefore, mapping the spatial distribution of forest density is essential for detecting changes driven by increasing anthropogenic pressures such as deforestation, road construction, settlement expansion, and rapid population growth over the past few decades (Cohen et al., 2017; Hadi et al., 2016; Ma et al., 2022; Popradit et al., 2015; Rodrigues et al., 2021). However, forest cover may be increasing in certain regions due to natural regeneration in previously disturbed areas (Crouzeilles et al., 2021; Palmero-Iniesta et al., 2021), for example, on coal mine lands in Jharkhand, India (Singh, 2021). To capture these changes systematically, forest canopy cover serves as a key metric, and advances in remote sensing have made its mapping more robust and reliable across large landscapes.

Forest canopy cover, also known as crown cover, is a fundamental parameter defined as the proportion of the forest floor covered by the vertical projection of the tree crowns (Korhonen et al., 2017). It is a significant indicator of forest conditions, influencing ecological processes such as light availability to the understory, microclimate regulation, and biodiversity (Pal et al., 2018; De Pauw et al., 2022; Lenk et al., 2024). Canopy density mapping is a vital tool used to assess and monitor this parameter over broad scales, offering a clear advantage in efficiency and coverage over traditional, labor-intensive field plots (Chandrashekhar & Roy, 2000). While field methods are essential for ground-truthing, remote sensing methods provide wall-to-wall data needed for large-scale analysis (Korhonen, 2011; Korhonen et al., 2006). Furthermore, while Light Detection and Ranging (LiDAR) provides valuable three-dimensional structural data on canopy height and volume, its application is often constrained by high costs, limited spatial coverage, and data availability (Erdody & Moskal, 2010; Korhonen et al., 2015). In contrast, canopy density mapping commonly utilizes passive optical sensors, which are widely available, cost-effective, and provide a reliable measure of forest canopy extent and density (Boutsoukis et al., 2019; Stojanova et al., 2010). This distinct perspective is invaluable for the implementation and development of afforestation and reforestation programs, and for identifying and monitoring forest health (Chandrashekhar et al., 2005; Kucsicsa et al., 2020; Santos et al., 2020). Recent methodological advancements, including the use of machine learning techniques such as artificial neural networks and random forest, have significantly improved the accuracy and efficiency of canopy density mapping, although their application can be constrained by the need for large training datasets, high computational requirements, and challenges in model transferability across different landscapes (Gyawali et al., 2024; Joshi et al., 2006). The International Tropical Timber Organization (ITTO) developed the Forest Canopy Density (FCD) model, a widely adopted methodology for quantifying canopy cover density (Palmero-Iniesta et al., 2021; Rikimaru & Koganei-shi, 2017). This model effectively identifies degrees of forest degradation and has gained acceptance among researchers as a reliable surrogate for estimating overall forest cover (López García et al., 2016).

The mineral-rich districts of Keonjhar and Sundargarh in Odisha have been experiencing significant forest degradation due to the rapid growth of mining and industrialization, posing a serious and ongoing threat to the region's moist-deciduous forests. While existing research has documented historical forest cover loss in the state (Mishra et al., 2022), a comprehensive, long-term assessment of canopy changes over this entire period has been absent. On this background, this study addresses this critical gap by first conducting a detailed, Landsat-based analysis of Forest Canopy Density (FCD) for the years 1988 and 2021. A trend analysis of the Normalized Difference Vegetation Index (NDVI) from 1988 to 2021 was then performed, using pixel-wise trends to identify and validate affected zones. This is essential for understanding the long-term forest dynamics influenced by such extensive anthropogenic pressure.

2. Methodology

2.1. Study area

The study area encompasses Keonjhar and Sundargarh districts in Odisha, situated along the eastern coast of India, covering approximately 17,952 km². Keonjhar is located between 21.01°N and 22.15°N latitudes, and 85.18°E and 86.37°E longitudes, while Sundargarh spans from 21.58°N to 22.53°N latitude and 83.53°E to 85.37°E longitude (Fig. 1). The region experiences a semi-arid climate, characterized by significant water scarcity during the summer months. The area includes several important forest tracts, such as the Kendujhar–Saranda range, the largest Sal forest belt; parts of the Harichandanpur–Telkoi forest, a lateritic plateau with thin, drought-prone soils; the Hemgir forest range, a steep upland iron-ore ridge; and the Bamra–Gangpur forest, a moist-deciduous zone bordering the Mahanadi basin. These forests are part of the Eastern Highlands Moist Deciduous Forests, which serve as vital wildlife habitats and corridors. The ecological significance of the region is underscored by the presence of rare fauna, such as the black

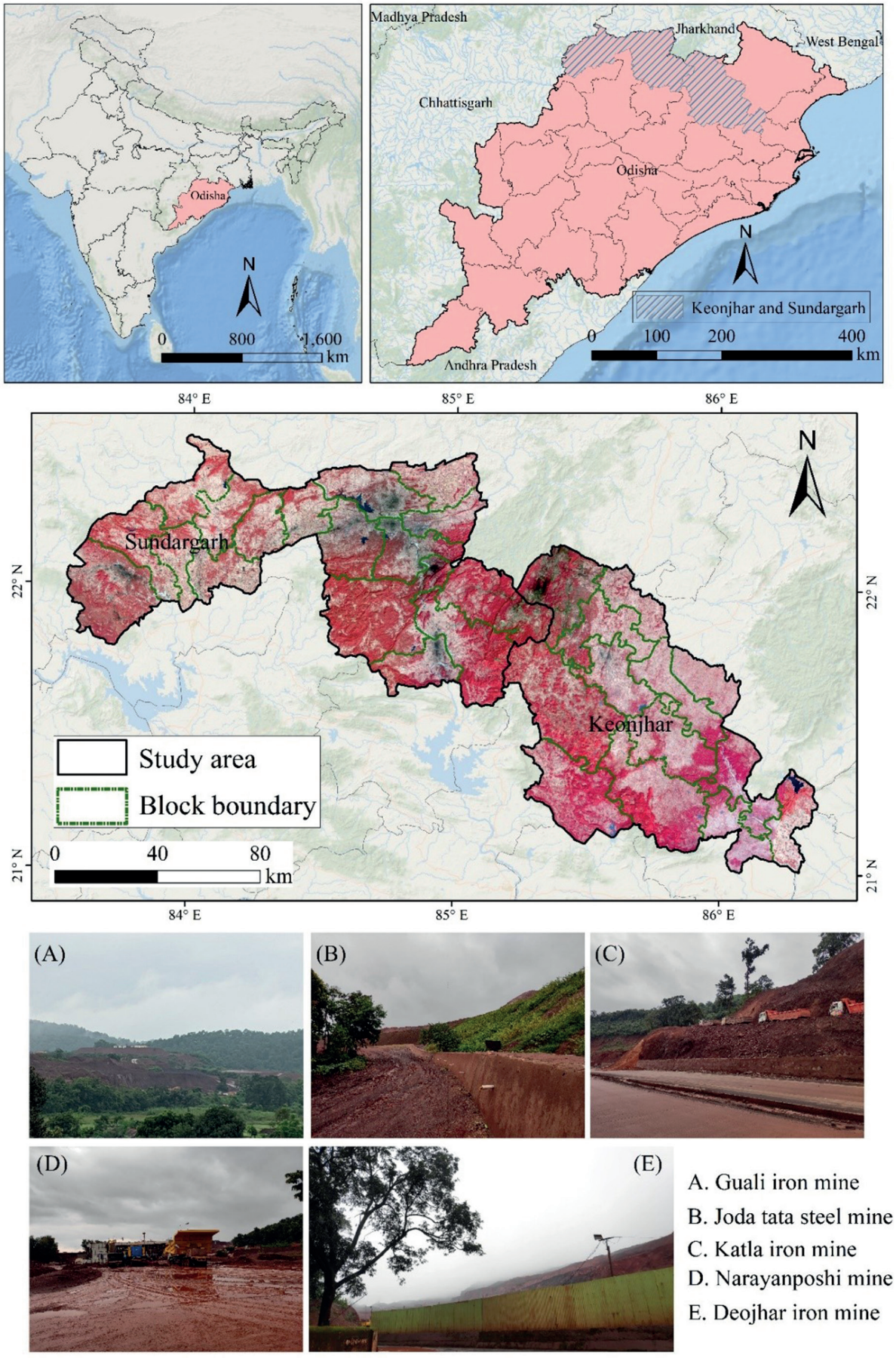

Figure 1. Location map of the study area and five mining areas from the study area photographed during the field visit: A. Guali iron mine, B. Joda Tata Steel mine, C. Katla iron mine, D. Narayanposhi mine, and D. Deojhar iron mine

panther in Hemgir, as well as recurring human-elephant conflict zones in Bamra–Gangpur.

Geologically, the region is part of the Mesoarchaean Iron Ore Group, which contains extensive mineral resources, including iron ore, manganese, limestone, dolomite, chromium ores, and recently discovered gold. This richness has established the area as a hub for mining and industrial development, with major steel plants, fertilizer units, cement factories, and glass manufacturing facilities situated here. However, unregulated mining and rapid industrialization have resulted in widespread deforestation, habitat fragmentation, and biodiversity loss. Additionally, these activities have exacerbated soil erosion, altered hydrological regimes, and increased air and water pollution due to emissions and mine waste. The cumulative impacts pose significant ecological challenges, rendering the region highly vulnerable and in urgent need of sustainable management strategies. Figure 1 illustrates the location of the study area and five selected mining sites—chosen from among numerous sites in the region—that were photographed during the field visit.

2.2. Datasets

LANDSAT data is among the most suitable and widely accepted datasets for understanding Earth's natural resources and land cover. The LANDSAT Thematic Mapper (TM) and Operational Land Imager (OLI) sensors provide seasonal coverage of global land cover at a spatial resolution of 30 meters, capturing visible, near-infrared (NIR), and shortwave infrared (SWIR) bands. These data are freely available from the United States Geological Survey (USGS). To analyze long-term variations in canopy density while minimizing the influence of phenological changes, the images should be acquired from the same season or month. LANDSAT surface reflectance images from February 1988 and February 2021 were used to assess spatio-temporal variations in forest canopy. For each year, median composite images were generated from February scenes with less than 10% cloud cover. All reflectance data were obtained from Google Earth Engine's surface reflectance collection, which has been pre-processed for atmospheric correction. Maps of roads, railways, settlements, mining areas, and industrial sites were utilized to delineate disturbance zones. For trend analysis, LANDSAT TM, ETM+, and OLI images spanning 1988 to 2021 were employed. Additionally, the MODIS Vegetation Continuous Fields (VCF) product was used to validate the forest canopy density map. The VCF provides surface vegetation cover data, i.e., percent tree cover, percent non-tree cover, and percent non-vegetated cover at a spatial resolution of 250 meters. These products are freely provided by USGS LP DAAC and are instrumental in characterizing vegetation land cover, thereby supporting vegetation modeling and monitoring applications.

2.3. Methods

2.3.1. Forest Canopy Density Model

Since the 1960s, researchers have utilized remote sensing data and various vegetation indices (VIs) to extract information about vegetation properties. These indices are valuable for assessing a wide range of parameters, broadly classified into structural (e.g., leaf area index, fractional green cover, canopy architecture) and biochemical (e.g., chlorophyll and water content) attributes (Kganyago et al., 2021; Verrelst et al., 2019; Xue & Su, 2017). Although VIs are sensitive to these parameters, many, such as the widely used Normalized Difference Vegetation Index (NDVI), exhibit non-linear responses, often reaching a saturation point in high-density canopies, which limits their sensitivity (Tian et al., 2025; Wang et al., 2016). This saturation phenomenon is a well-documented challenge that affects numerous vegetation indices (Yang et al., 2007). In this study, the Forest Canopy Density (FCD) model was employed, utilizing the Advanced Vegetation Index (AVI), Bare Soil Index (BI), and Shadow Index (SI), specifically formulated for this model to quantify changes in forest canopy density. The multi-index approach enhances robustness by combining the complementary strengths of AVI, BI, and SI to characterize different aspects of the forest canopy. Notably, the SI maintains sensitivity in dense stands where other indices tend to saturate, providing a more accurate assessment of canopy density. Figure 2 presents the methodological workflow.

The methodology for assessing Forest Canopy Density (FCD) was developed as part of the ITTO project titled "Rehabilitation of Logged-over Forests in the Asia-Pacific Region, Sub-project III". This approach enables the measurement of deforestation over time as well as the evaluation of reforestation progress (Bhandari & Nandy, 2024; Rikimaru et al., 2002). The model is based on changes in vegetation density, utilizing a combination of biophysical indices to characterize forest conditions. A healthy forest is represented by dense canopies and corresponds to high FCD values, whereas areas with sparse or absent canopies indicate degradation or deforestation (Rikimaru & Miyatake, 2009). The Advanced Vegetation Index (AVI) is particularly effective in detecting subtle differences in canopy density, leveraging the degree of infrared response (Loi et al., 2017). The Bare Soil Index (BI) was used to identify areas of bare soil or fallow land, as it relies on medium infrared data; the index value increases with the degree of land uncovered or soil exposure (Kumar et al., 2015). Given that the study

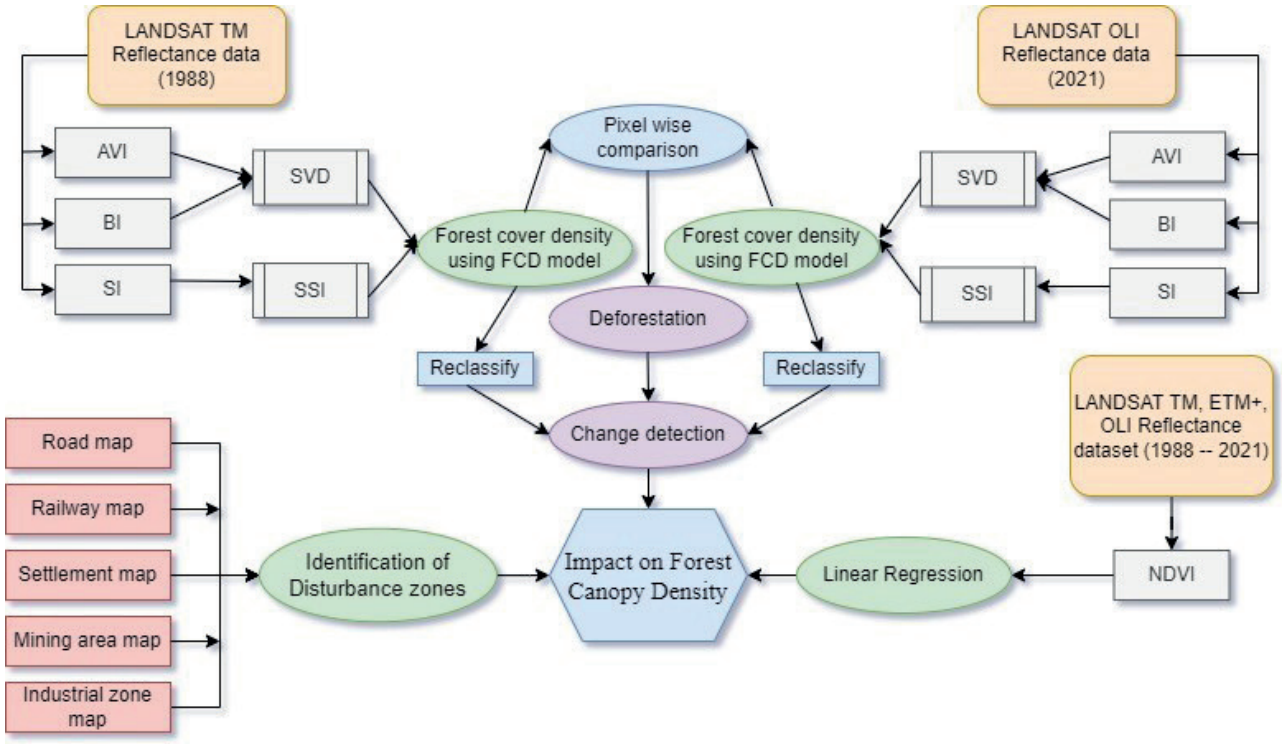

Figure 2. Flowchart of the methodology

area is characterized by hilly terrain, it is also essential to account for shadow effects. The Shadow Index (SI), which captures spectral information related to canopy shadows, is vital for analyzing the thermal properties and structural characteristics of the forest, especially in complex topography.

Advanced Vegetation Index (AVI): AVI is one of the important parameters to detect healthy vegetation. It highlights the subtle difference in canopy density, whether the density is high or low, using red and near-infrared spectral bands (Himayah et al., 2016; Syakur et al., 2025). AVI is calculated using the following formula (eq.1):

$$AVI = [(NIR + 1)(256 - R)(NIR - R)]^{\frac{1}{3}} \quad (1)$$

For OLI, 256 will be 65536. AVI = 0 if, IR < R, after normalization.

Bare Soil Index (BI): Bare soil refers to soil or sand that is not covered by any vegetation. In areas with sparse vegetation cover, standard vegetation indices often struggle to accurately represent ground conditions. To obtain more precise information about forest status and soil characteristics, the Bare Soil Index (BI) is widely employed. It is also useful for distinguishing between agricultural and non-agricultural lands (Abdollahnejad et al., 2017). BI is calculated using the following formula (eq.2):

$$BI = \frac{(SWIR+R)-(NIR+B)}{(SWIR+R)-(NIR+B)} \times 100 + 100 \quad (2)$$

Scaled Vegetation Density (SVD): Vegetation density (VD) is derived from Principal Component Analysis (PCA) applied to the AVI and BI indices, which are significantly negatively correlated. PCA transforms a set of correlated variables into uncorrelated principal components, with the first component (PC1) capturing the maximum variance in the data (Kherif & Latypova, 2020). The VD is defined as the score of PC1, which can be expressed as a linear combination of the original indices (eq. 3):

$$VD - a.\,AVI + b.\,BI \quad (3)$$

where, the coefficients a and b are the loadings from the eigenvector corresponding to the largest eigenvalue of the data's covariance matrix, represent the weights determining each index's contribution to the new composite axis.

Since the raw VD values obtained from PCA are not standardized and can be difficult to interpret or compare directly, the PCA results are scaled to a range of 0 to 100, resulting in the Scaled Vegetation Density (SVD) (eq. 4).

$$SVD = \frac{VD - VD_{min}}{VD_{max} - VD_{min}} \times 100 \quad (4)$$

This normalization makes the SVD values easily interpretable, with 0 indicates minimal vegetation density corresponding to bare soil, while 100 denotes the maximum vegetation density.

Shadow Index (SI): Forests are inherently three-dimensional structures characterized by the horizontal and vertical arrangement of trees, shrubs, and other vegetation components, along with non-living elements such as soil and terrain features (Seidler & Bawa, 2001). The SI is designed to evaluate variations in canopy shadow patterns that influence spectral response, which are affected by factors such as forest structure, age, and species composition. This index is derived by analyzing low radiance signals captured in the visible bands (Deka & Tripathi, 2013; Mon et al., 2012). Areas with sparse vegetation or agricultural lands tend to exhibit low canopy shadow indices, whereas dense or medium-dense forests display higher SI values. SI is calculated using the following formula (eq.5):

$$SI = [(256 - B)(256 - G)(256 - R)]^{\frac{1}{3}} \quad (5)$$

For OLI surface reflectance images, 256 will be 65536.

Scaled Shadow Index (SSI): The SSI quantifies the spectral differences associated with mature or fully developed forests, which exhibit higher canopy shadow indices. It is calculated through a linear transformation of the Shadow Index (SI), with a scale ranging from 0 to 100; where 0 indicates the lowest shadow area (0%) and 100 signifies the highest shadow area (100%).

Forest Canopy Density (FCD): FCD is derived by integrating the SSI and Scaled Vegetation Density (SVD), and it is expressed on a scale from 1 to 100. FCD is calculated using the following formula (eq.6):

$$FCD = [(SVD \times SSI) + 1]^{\frac{1}{2}} - 1 \quad (6)$$

To validate the accuracy of FCD estimates, the derived values were compared with the MODIS Vegetation Continuous Field (VCF) product available for the region. Approximately 100 random points were selected across the study area, and FCD values were extracted from both datasets for subsequent comparison and analysis.

2.3.2. Deforestation and change detection

Forested areas were delineated from the FCD map and reclassified following FSI guidelines into four categories: dense forest (>70%), moderately dense forest (40–70%), open forest (10–40%), and non-forest. Change detection was performed by comparing bi-temporal images, generating a map with nine classes reflecting different transition states. The map was represented by nine categories based on forest density: dense forest to moderately dense forest, dense forest to open forest, moderately dense forest to dense forest, moderately dense forest to open forest, open forest to moderately dense forest, unchanged category in three classes, and deforestation (forest to non-forest).

2.3.3. Disturbance zone mapping

A disturbance zone map was created using Google Earth imagery from 2020. Features such as highways, roads, railways, industrial sites, settlements, and mining areas were manually digitized. These features were geometrically corrected using polynomial transformations and projected into the UTM coordinate system to ensure spatial accuracy. To capture their relative ecological impacts, several buffers were established around each feature to quantify their ecological impact: 500 m for mines (to account for excavation, dumps, and settlement expansion), 100 m for settlements (to represent population growth due to mining), 500 m for industrial sites (reflecting large footprints and waste areas), 50 m for highways and railways (acknowledging localized but comparatively smaller effects) and 20 m for other roads. Overlapping buffers were merged to delineate the composite disturbance area. The final map was validated through field surveys, which confirmed the reliability of the mapped disturbance patterns.

2.3.4. Long-term trend analysis

Forest degeneration and regeneration over a long period can be detected by the temporal trend analysis (Eckert et al., 2015; Vancutsem et al., 2021). Long-term trends of forest degradation and regeneration were analyzed via temporal trend analysis of NDVI, by using its extensive historical record from Landsat sensors. NDVI's consistent calculation and widespread validation make it a robust metric for monitoring vegetation dynamics over decades (Forkel et al., 2013; Gillespie et al., 2018; Jamali et al., 2015; Ju & Masek, 2016; Martínez & Gilabert, 2009; Plessis, 1999; Sharma et al., 2021; Xiong & Wang, 2022; Zoungrana et al., 2018). The analytical approach involved pixel-wise linear regression of NDVI over time, treating time as the independent variable and NDVI as the dependent variable (Tian et al., 2015). The slope (β) of the regression line reflects the average annual rate of NDVI change per pixel, serving as an indicator of long-term vegetation gain or loss. A low slope indicates minimal or no change, whereas a high positive or negative slope indicates significant vegetation increase or decline, respectively. This trend analysis was conducted using the R programming language. The period analyzed spanned from 1988 to 2021, utilizing 33 annual NDVI layers. These layers were created by generating median composites from Landsat surface reflectance data prior to NDVI calculation, ensuring consistency and minimizing the influence of transient seasonal effects. The slope was spatially mapped to visualize long-term vegetation dynamics across the study area (eq. 7).

$$SLOPE\ (\beta) = \frac{n\sum_{i=1}^{n} i \times image_i - (\sum_{i=1}^{n} i)(\sum_{i=1}^{n} image_i)}{n\sum_{i=1}^{n} i^2 - (\sum_{i=1}^{n} i)^2} \quad (7)$$

where n indicates the studied years; i indicates the serial number of the year, and image i is the image (NDVI) value of the year i.

3. Results

3.1. Forest cover density

The comparison of the Advanced Vegetation Index (AVI) between 1988 and 2021 reveals a significant decline in dense vegetation cover across Keonjhar district, particularly in its northern regions. This trend is primarily driven by extensive mineral extraction activities, which have led to the conversion of forested land into bare surfaces.

The Bare Land Index (BI) corroborates this observation, showing a corresponding rise in bare land areas during the same period, especially in zones where canopy cover has been markedly reduced. Concurrently, the Spectral Index (SI) values exhibit a downward trend from 1988 to 2021, reflecting a decline in vegetation density. The most notable decreases in SI were observed in grasslands, agricultural fields, and vacant lands, compared to relatively stable or less impacted forested zones. While the overarching trend indicates widespread forest degradation, localized signs of regeneration are evident in older mining sites and patches previously classified as bare land. These areas show modest recovery, suggesting ongoing successional processes post-disturbance. Spatial distribution maps of AVI, BI, and SSI (Figs 3 and 4) illustrate these temporal changes, emphasizing the spatial variability of vegetation dynamics over the three decades.

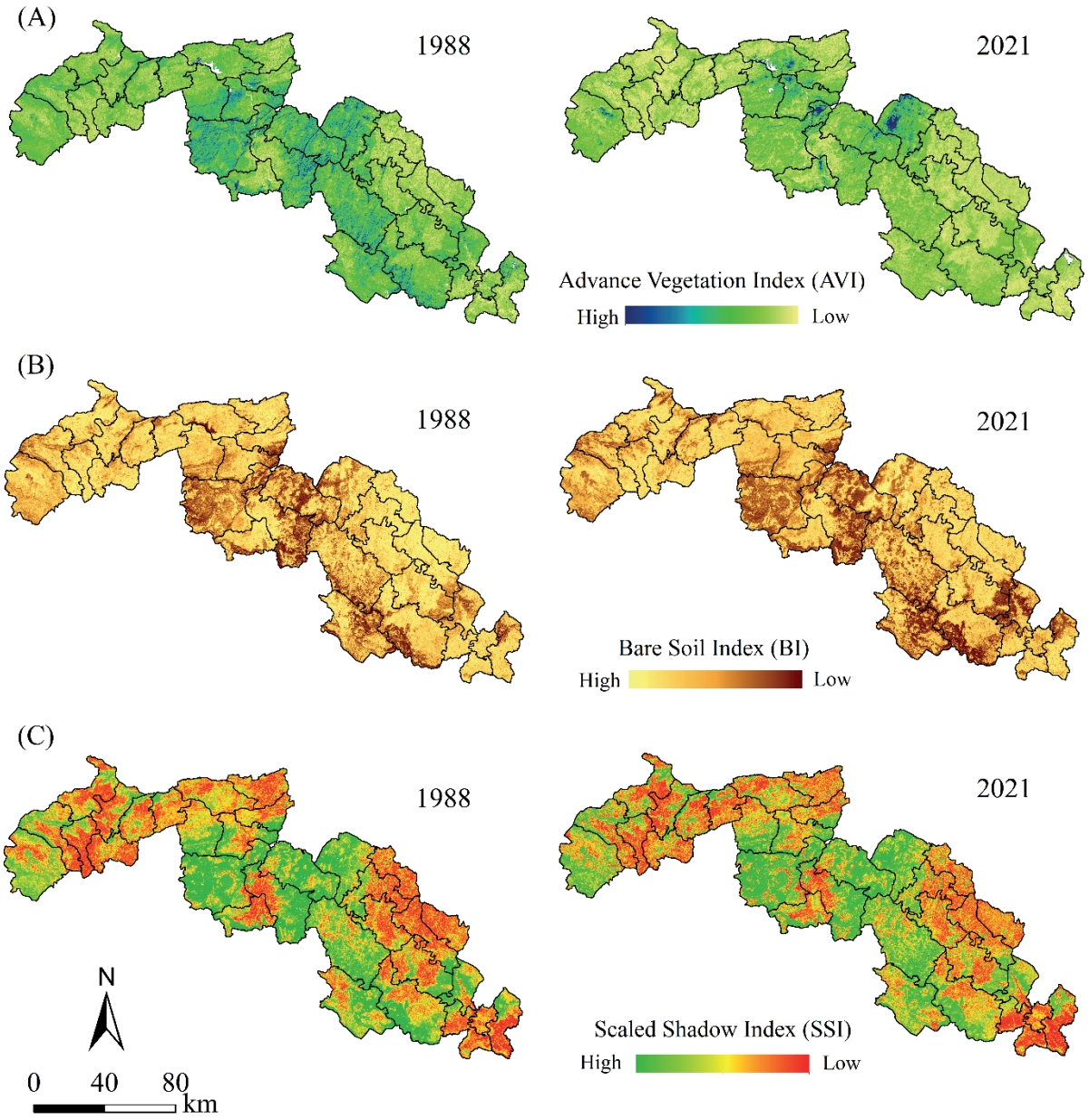

Figure 3. (A) AVI maps of 1988 and 2021, (B) BI maps of 1988 and 2021, (C) SSI maps of 1988 and 2021

Quantitative analysis indicates that forest cover in Keonjhar declined from 3,640.53 km² (44.06% of the district) in 1988 to 3,135.73 km² (37.95%) in 2018, representing a net loss of approximately 504.80 km² or 6.11%. The most affected categories were moderately dense and open forests, which decreased by 272.12 km² (−3.29%) and 316.83 km² (−3.83%), respectively. Interestingly, dense forest patches showed a slight but notable increase (+56.20 km², +0.68%), likely reflecting the persistence of core forest areas less impacted by anthropogenic activities. Extending the analysis to 2021 reveals that dense forest cover further declined by nearly 9% in the Joda, Koida, and Lahunipara blocks, predominantly due to the transformation of medium-density forests into open forests and bare land. Additionally, approximately 15% of the open forest along forest edges was converted into bare land, although some areas exhibited minor recovery, with about 6% of forest cover increasing in the Anandapur, Harichandanpur, and Telkoi regions.

Similarly, Sundargarh district experienced deforestation, with forest cover decreasing from 4,655.74 km² (48.05%) in 1988 to 4,257.39 km² (43.94%) in 2018, a net loss of 398.35 km² or 4.11%. The most significant reduction occurred in dense forests (−267.61 km² or −2.76%), while moderately dense forests expanded slightly (+66.84 km² or +0.69%), possibly reflecting re-growth or regeneration in certain zones. Open forests saw a considerable decrease (−195.51 km² or −2.02%) over this period. Between 1988 and 2021, medium forest cover increased by nearly 3% in the Gurundia, Rajganjpur, and Lephripara blocks, although other areas such as Bisra, Rajganjpur, and Lahunipara showed pronounced forest loss. Figure 5 illustrates the changes in forest cover at the block level.

At the broader landscape scale, the combined forest cover across both districts diminished from 8,263.15 km² in 1988 to 7,333.90 km² in 2018, corresponding to a net loss of 929.25 km² or 5.18%. The most substantial reductions were observed in open forests (−512.65 km²), followed by dense (−211.56 km²) and moderately dense forests (−205.04 km²). These changes are most pronounced in the Joda, Bansapal, Ghatagaon, Koida, Bisra, Rajganjpur, and Lahunipara blocks. Spatial maps of FCD (Fig. 4) and summary statistics (Table 1) provide further insights into the extent and spatial distribution of forest loss over this period.

Figure 6 depicts the spatial distribution of forest cover change phenomena within the study area, while Figure 7 illustrates the corresponding percentage changes over the period from 1988 to 2021. The analysis reveals that approximately 42% of forested pixels experienced class transitions during this period, highlighting significant landscape dynamics influenced by various anthropogenic activities, notably mining and industrial expansion. Among these transitions, 9% of dense forest pixels shifted to

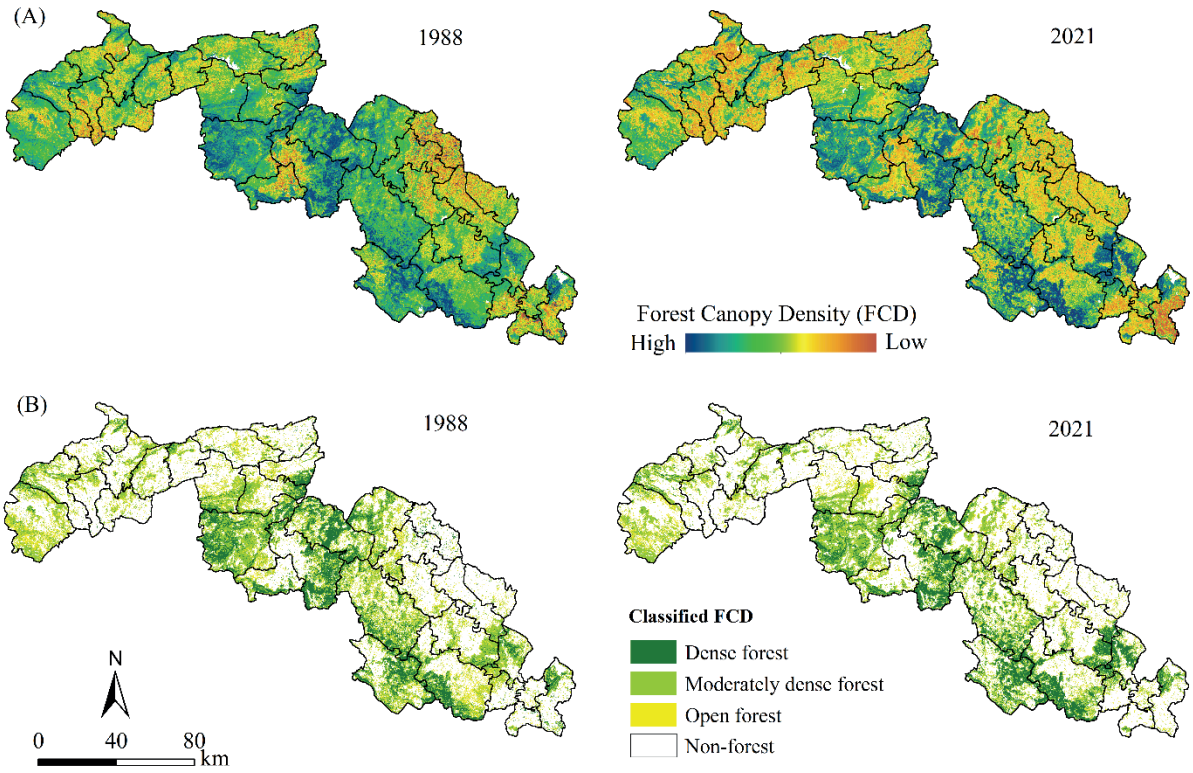

Figure 4. (A) FCD maps of 1988 and 2021, (B) Classified FCD maps of 1988 and 2021

Table 1. Forest and Non-forest area in Keonjhar and Sundargarh districts in the years 1988 and 2021

		Dense forest		Moderately dense forest		Open forest		Total forested area		Non-forest	
		Area (km^2)	%	Area (km^2)	%	Area (km^2)	%	Area (km^2)	%	Area (km^2)	%
1988	Keonjhar	930.88	11.27	1594.19	19.29	1115.46	13.50	3640.53	44.06	4621.96	55.94
2018		987.08	11.95	1322.07	16.00	798.63	9.67	3135.73	37.95	5126.76	62.05
Change		56.20	0.68	-272.12	3.29	-316.83	3.83	-504.80	6.11	504.80	6.11
1988	Sundargarh	1258.07	12.98	2033.81	20.99	1329.89	13.73	4655.74	48.05	5033.77	51.95
2018		990.46	10.22	2100.65	21.68	1134.38	11.71	4257.39	43.94	5432.12	56.06
Change		-267.61	2.76	-66.84	0.69	-195.51	2.02	-398.35	4.11	398.35	4.11
1988	Total	2189.10	12.19	3628.39	20.21	2445.66	13.62	8263.15	46.03	9688.65	53.97
2018		1977.54	11.02	3423.35	19.07	1933.01	10.77	7333.90	40.85	10618.10	59.15
Change		-211.56	1.18	-205.04	1.14	-512.65	2.86	-929.25	5.18	929.45	5.18

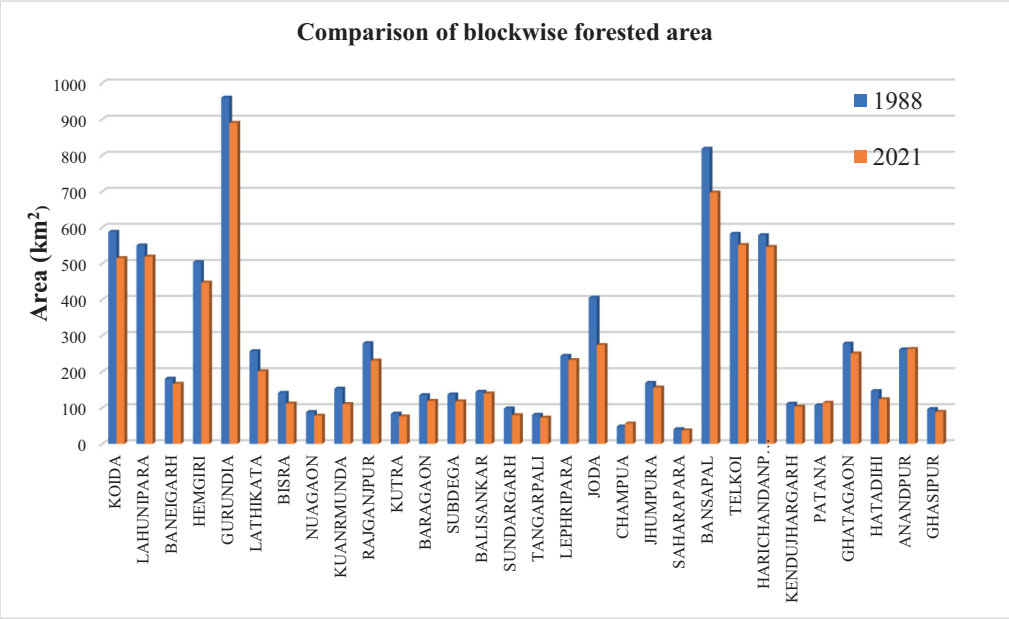

Figure 5. Comparison of block-wise forested areas (1988 and 2021)

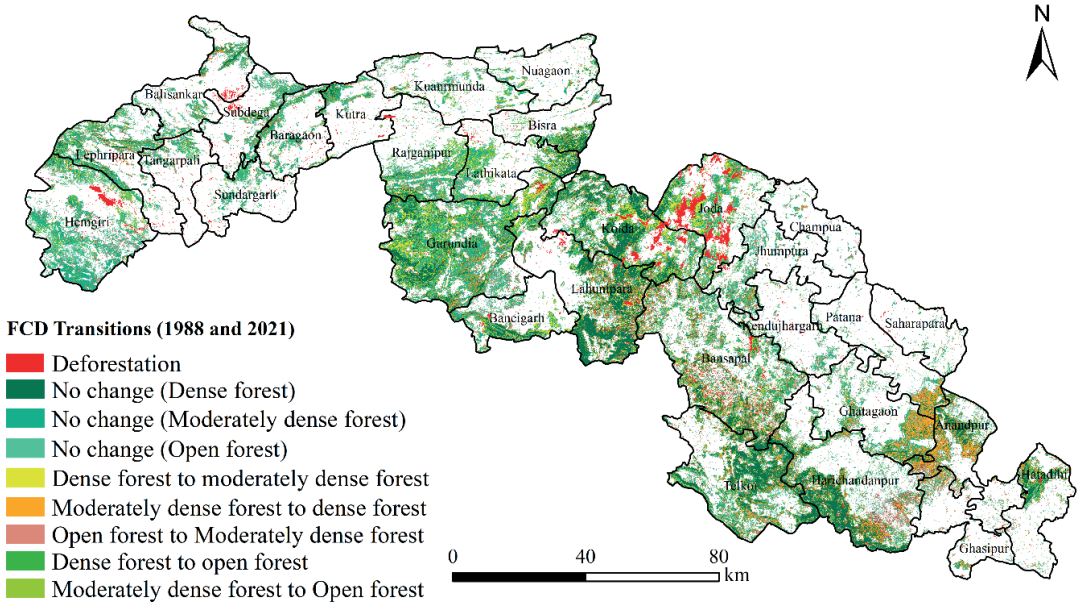

Figure 6. Change detection map of the forested area (from 1988 to 2021)

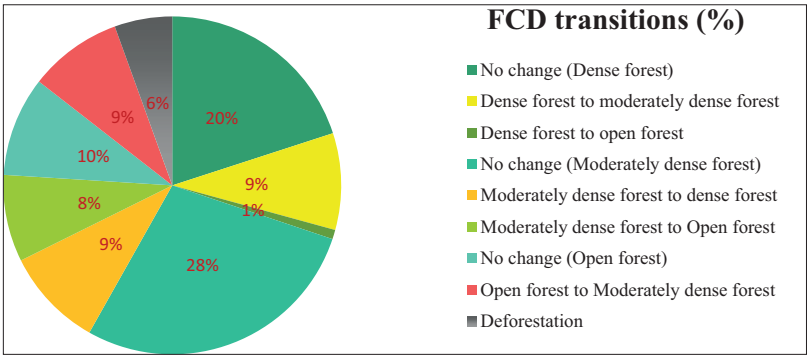

Figure 7. Percentage of changes in different forest classes

moderately dense forest, predominantly in the Joda, Banspal, Lahunipara, Koida, Bisra, Lathikata, Gurundia, Hemgir, and Rajganjpur blocks. These regions are characterized by intensive mining operations and industrial development, which have substantially altered the forest structure. Previous studies (Krishna et al., 2020) have linked such land use changes to the proliferation of steel and sponge iron industries concentrated in Joda and Koida, emphasizing the profound impact of industrialization on forest dynamics. Additionally, about 8% of moderately dense forest pixels degraded into open forest, indicating ongoing forest thinning and land degradation across the study area. Interestingly, localized regeneration activities were observed in specific regions: portions of moderately dense and open forests in the Telkoi, Anandpur, Harichandanpur, and Ghatagaon forest ranges exhibited signs of recovery, primarily driven by reforestation initiatives and plantation efforts. These positive trends suggest the potential for ecological restoration in areas where conservation measures are actively implemented. Overall, deforestation accounted for approximately 6% of the total forest area, with the most significant losses occurring within Keonjhar district—particularly in Joda and Banspal blocks—and Sundargarh district, especially in Koida, Lahunipara, Balisankar, and Hemgiri blocks. In Sundargarh, industrial expansion has played a crucial role in driving forest loss, especially in the Rajganjpur, Lathikata, and Bisra blocks, which have experienced notable increases in mining activity (Kumar et al., 2012; Lohchab & Saini, 2018). Figure 8 illustrates the distribution of disturbance zones within the study area, highlighting regions of intense anthropogenic pressure. Areas with negative slope values in the terrain correspond to zones of forest disturbance, where rapid land cover transformation is evident.

3.2. Trend analysis

In Keonjhar, the Joda and Bansapal blocks exhibit the highest negative slope trends, reflecting ongoing deforestation driven

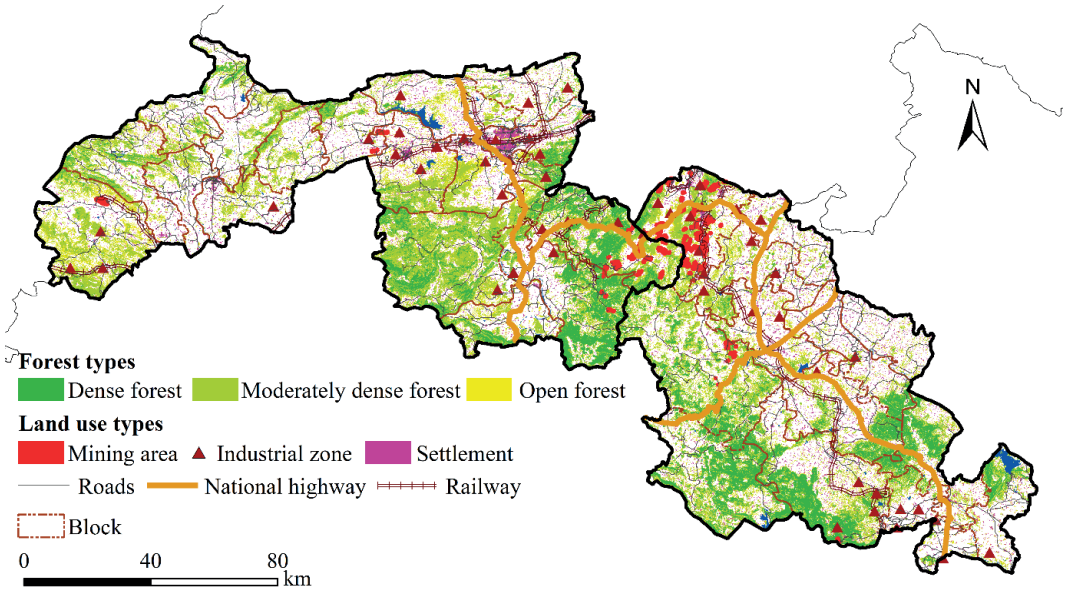

Figure 8. Human interferences in the forested areas of Sundargarh and Keonjhar districts

by extensive mining activities. Joda, a highly urbanized and industrialized city, is a prominent hub for iron and manganese mining, with suburban and urban expansion contributing to forest clearing. Despite ongoing deforestation, traces of reforestation and afforestation efforts are observable due to planned urban development strategies. Bansapal and Kendujhargarh also show negative trends, attributable to mining and urbanization. Conversely, regions such as Telkoi, Anandpur, and Harichandanpur reveal positive slope trends consistent with successful reforestation and plantation initiatives aimed at ecological restoration. In Sundargarh district, multiple blocks including Koida, Lahunipara, Kutra, Hemgiri, Gurundia, Kuanrmunda, Nuagaon, Rajagangapur, and Bisra exhibit negative slope trends, mainly due to extensive mining and industrial activities. Koida stands out with over 100 active mining sites for iron and manganese ores and hosts major industrial groups such as the Rungta, S.R., and Adhunik groups, which have substantially altered the landscape. Lahunipara and Gurundia also contain significant mineral deposits, including iron and manganese, contributing to ongoing land degradation. Additionally, limestone deposits in Nuagaon, Rajagangapur, Kutra, and Kuanrmunda, along with coal mines in Hemgiri, further intensify land use changes. Urbanization has accelerated in Bisra in recent years, further exacerbating forest loss. Figures 9 and 10 provide a detailed visualization of the NDVI trend analysis from 1988 to 2021 and the block-wise distribution of slope values, respectively. The NDVI analysis depicts areas of persistent vegetation decline, especially in mineral-rich zones, whereas the slope map highlights terrain-related vulnerabilities to land degradation. The combined insights emphasize the complex interplay between industrial activities and natural land cover changes, reflecting both the challenges and opportunities for sustainable forest management and ecological restoration in the region.

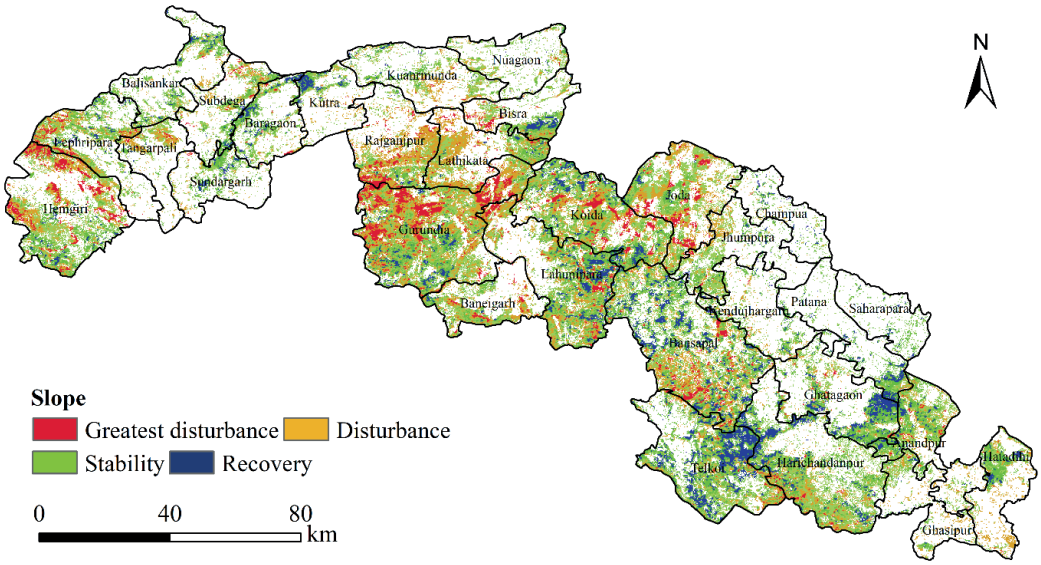

Figure 9. Trend analysis map of NDVI from 1988 to 2021

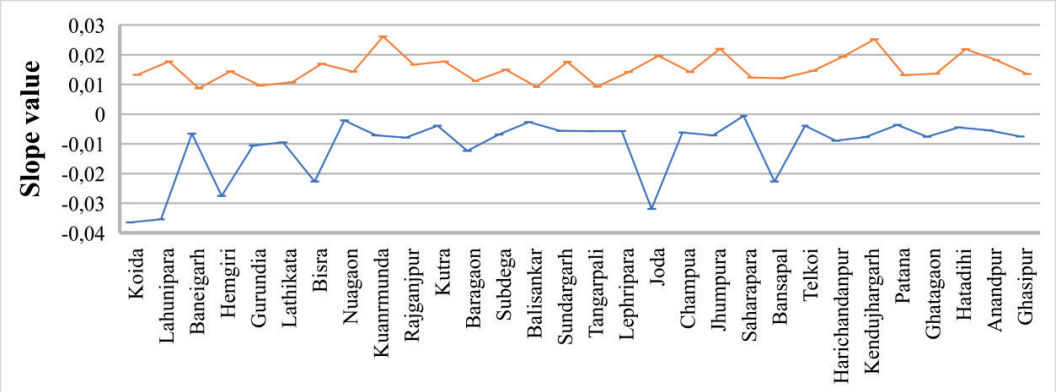

Figure 10. Block-wise ranges of slope value

3.3. Comparison of the MODIS VCF product and Forest Canopy Density map of 2021

To validate the Forest Canopy Density (FCD) model results, we employed the MODIS Vegetation Continuous Field (VCF) product as a reliable reference dataset. A total of 100 randomly selected points across the forested regions within the study area were established for this purpose. The values of canopy cover density extracted from the FCD model were correlated with the corresponding values obtained from the MODIS VCF product. The correlation analysis yielded a coefficient of determination (R^2) of 0.73, which was statistically significant at $p < 0.01$, indicating a robust agreement between the two datasets. This high correlation underscores the reliability of the FCD model in accurately representing forest canopy conditions (Figs 11 and 12).

The utility of canopy cover mapping extends beyond mere forest health assessment; it is instrumental in guiding policy formulation and implementing forest management programs aimed at sustainable development (Godinho et al., 2016; Fasil et al., 2022). Conversely, extensive canopy cover loss poses a severe threat to ecosystem stability, primarily driven by anthropogenic activities such as urban expansion, industrialization, and mineral extraction (Hoang & Kanemoto, 2021).

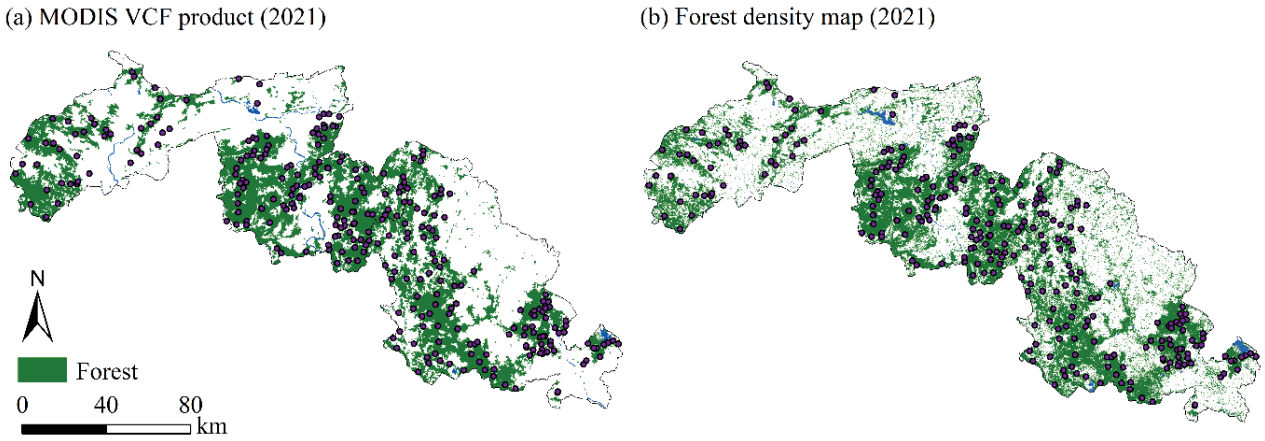

Figure 11. (a) MODIS VCF product of 2021, and (b) FCD map of 2021

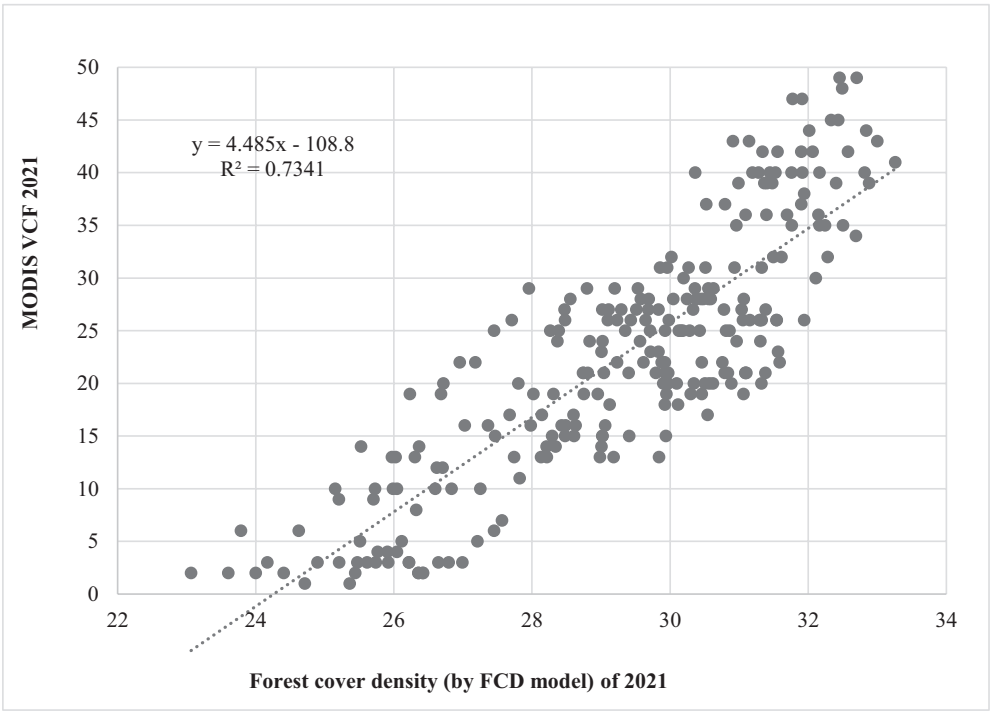

Figure 12. Correlation between MODIS VCF 2021 and FCD 2021

4. Discussion and Conclusions

4.1. Discussion

In this study, long-term changes in canopy cover density were analyzed over the period from 1988 to 2021, employing the FCD model integrated with multiple spectral indices, namely the Average Vegetation Index (AVI), Brightness Index (BI), and Shadow Index (SI). A notable limitation of traditional vegetation indices (VIs) is saturation in dense forest conditions, where these indices plateau, failing to detect additional canopy growth or decline (Gao et al., 2023; Wang et al., 2023; Zhang et al., 2023). To overcome this, the FCD model incorporates the Shadow Index, which intensifies with increasing canopy density as shadows deepen, providing a more sensitive measure of dense forest structure (Ismail et al., 2017; Prodromou et al., 2022). This multi-index approach enhances the robustness and reliability of the model, particularly in densely forested regions, thus increasing confidence in the reported temporal changes in forest cover within Odisha.

The analysis reveals substantial forest disturbances in two of Odisha's key mineral-rich districts, Keonjhar and Sundargarh. Our findings indicate that approximately 211 km² of dense forest cover was lost over the study period, predominantly in core forest zones and their peripheries. This loss is primarily linked to escalating mining activities, which drive extensive clearing of forestland to accommodate mineral extraction operations. Mining-related processes generate considerable dust emissions, escalate transportation infrastructure development, and necessitate road construction, all of which contribute to accelerated deforestation, especially at forest margins and in surrounding landscapes.

These results are consistent with broader historical trends of deforestation across Odisha. According to historical records, from 1935 to 2010, the state experienced a net decrease of approximately 40.5% in forest cover, translating to an average annual deforestation rate of 0.69% (Sudhakar Reddy et al., 2018). More recent satellite-based assessments and global forest monitoring platforms indicate that Odisha lost around 1,470 km² of tree cover between 2001 and 2024 (https://www.globalforestwatch.org/dashboards/country/IND/26/?category=forest-change). Specifically, in Keonjhar district alone, the loss amounted to approximately 59.7 km² of forest cover during this period, with a recent government report revealing that 64 mining projects have diverted 104.51 km² of forest land over the past 38 years—the highest in any district within Odisha since 1980 (https://india.mongabay.com/2019/09/tribal-way-of-life-hits-rock-bottom-even-as-mining-hits-new-highs-in-odisha/). Multiple studies have further reinforced these observations; for example, Mishra et al. (2022) reported that between 2000 and 2018, Keonjhar experienced a loss of 111.91 km² of forest cover, while Sundargarh lost 34.87 km² in the same timeframe. Hota and Behera (2015, 2016, 2019) provided a comprehensive assessment of mining-induced pressures across Odisha, highlighting that approximately 99% of the state's mineral value is concentrated in districts such as Angul, Jajpur, Jharsuguda, Keonjhar, Koraput, and Sundargarh. Keonjhar alone harbors nearly one-third of Odisha's mineral reserves, and together with Sundargarh, these districts contribute over 50% of the state's total mineral wealth. The analysis further indicates a marked increase in the production of chromite, coal, iron ore, and bauxite over the study period, while manganese mining showed a notable decline (Hota & Behera, 2019). These mineral extraction activities, in conjunction with expanding infrastructure and urbanization, continue to exert immense pressure on Odisha's forests, leading to persistent degradation and fragmentation of forest ecosystems.

Beyond the quantifiable loss of forest area, the ecological consequences of forest fragmentation command particular concern due to their profound impacts on biodiversity, ecosystem stability, and resilience. Long-term landscape analyses reveal that forest fragmentation in Odisha has intensified markedly over the past century. Specifically, the number of forest patches per 1,000 square kilometers increased dramatically from 2.463 in 1935 to 15.102 in 2010, demonstrating a near sixfold rise in fragmentation. Concurrently, the average patch size diminished substantially from approximately 33.2 km² to a mere 3.2 km² (Sudhakar Reddy et al., 2018). These shifts highlight a transition towards a landscape characterized by numerous small, isolated forest fragments, which significantly compromises ecosystem integrity and functions. Ecologically, fragmentation impacts are far-reaching. A reduction in contiguous forest habitat leads to habitat loss for wildlife species, resulting in population declines and increased extinction risks, especially for specialized and endemic species that depend on interior forest conditions. Fragmentation also severs gene flow among populations, heightening the likelihood of inbreeding depression and reducing genetic diversity, which diminishes overall adaptability to environmental changes (Hermes et al., 2016; Ramsay et al., 2023). Moreover, as forests become more fragmented, they develop increased edge habitats. These edge zones experience altered microclimatic conditions such as higher temperature fluctuations, increased light penetration, and wind exposure, which favor generalist and invasive species over native forest interior specialists (Ewers & Banks-Leite, 2013; Magnago et al., 2015; Pfeifer et al., 2017). This shift can lead to a decline in biodiversity and disrupt ecosystem functions such as pollination, seed dispersal, and nutrient cycling.

In our current study, the loss of approximately 929.25 km² of forest cover further illustrates the severity of ecological decline. This numeric reduction is not merely a measure of spatial contraction; it signifies a deterioration in ecological health and system resilience attributed to fragmentation processes. To reinforce these findings, Normalized Difference Vegetation Index (NDVI)-based trend analyses were employed to assess spatial variations in forest canopy dynamics across different administrative blocks. The resulting spatial maps of slope values reveal that regions exhibiting negative trends; indicative of canopy decline correlate strongly with known hotspots of mining and industrial activity. This spatial concordance confirms that anthropogenic pressures are primarily responsible for the observed degradation rather than natural variability. Conversely, some regions display positive NDVI trends, associated with reforestation initiatives, afforestation, or plantation programs, thereby illustrating potential areas of recovery. These complementary analyses enhance the robustness of the FCD model's ability to detect both degradation and regeneration processes, providing vital insights for targeted conservation efforts and adaptive forest management.

The deterioration of forest canopy density in Keonjhar and Sundargarh districts is attributable to an intricate web of human activities, with mining and associated industrialization acting as primary drivers. Mining exerts both direct and indirect ecological pressures. Directly, it involves the physical clearing of vast tracts of forested land to establish pits, waste dumps, and processing facilities, leading to permanent loss of vegetation cover. Indirectly, mining catalyzes extensive infrastructure development, especially road networks, which fragment forests, enabling further encroachment for agriculture, settlement, and illegal extraction activities. These roads facilitate human access, exacerbate habitat disturbance, and elevate risks of human-wildlife conflicts and vehicle collisions.

Urbanization, though often considered a secondary driver globally, plays a significant localized role in districts like Keonjhar and Sundargarh. Urban expansion alters land cover, increases impervious surfaces, and modifies hydrological regimes. Such changes intensify surface runoff, soil erosion, and local temperature increases (urban heat islands). Additionally, urban development often promotes deforestation for infrastructure and housing, while diverting agricultural lands for urban use can trigger compensatory deforestation elsewhere, contributing further to landscape fragmentation (Basu & Nayak, 2011; Kumar, 2014; Mishra, 2010; Mishra & Pujari, 2008). The cumulative effect of mining, industrial growth, and urban expansion creates a reinforcing cycle that accelerates forest loss and fragmentation, thereby undermining the ecological stability of Odisha's resource-rich districts.

Collectively, these findings reveal that forest degradation in Keonjhar and Sundargarh transcends simple area loss; it involves profound structural and functional transformations of the forest landscape. The combined impacts of mining-induced industrialization and localized urban expansion result in extensive deforestation, fragmentation, and habitat degradation. These changes threaten biodiversity through habitat loss and altered community compositions, compromise ecosystem services, including carbon sequestration, soil fertility, and water regulation and jeopardize the long-term sustainability of forest ecosystems. Addressing these challenges warrants integrated land-use planning, sustainable mining practices, and active forest restoration efforts to safeguard ecological integrity. Importantly, the synergy of long-term remote sensing analyses combining multi-index FCD modeling, NDVI trend mapping, and spatial pattern analysis provides a comprehensive framework to monitor, understand, and mitigate ongoing forest fragmentation in Odisha, ensuring informed conservation strategies in the face of rapid developmental pressures.

4.2. Conclusion

Analysis of forest canopy density in Keonjhar and Sundargarh districts from 1988 to 2021 reveals a significant decline in forest health, primarily driven by anthropogenic pressures. Using the Forest Cover Density (FCD) model, our results show a loss of 416.6 km² of dense and moderately dense forest cover over this period. Conversely, only a minimal proportion of open and degraded forests showed signs of regeneration, indicating that natural recovery processes are insufficient to counterbalance ongoing loss. Notably, 211 km² of dense forest was lost, with the most severe impacts concentrated around mining clusters such as Joda, Koida, Lahunipara, and Rajagangpur. This spatial pattern aligns with the proximity of forests to active mining leases, industrial complexes, and related infrastructure, which our disturbance parameter analysis confirms. A high proportion of forest pixels within 500 meters of such development shifted from denser classes to open or bare land, underscoring mining expansion, industrialization, road construction, and settlement growth as primary drivers of deforestation.

These observed patterns are consistent with global trends of increasing fragmentation and shrinking core forest areas, as reported by Hansen et al. (2020). In Keonjhar and Sundargarh, fragmentation has accelerated, resulting in smaller, isolated patches that diminish habitat continuity and resilience. Such fragmentation exacerbates edge effects, facilitates the invasion of non-native species, and accelerates biodiversity decline, undermining ecosystem stability. While mining remains critical for regional development,

its ecological impacts can be mitigated through stricter regulatory enforcement, adoption of environmentally sustainable technologies, and active ecological reclamation of mined lands. Practices like concurrent reclamation, dust suppression, water treatment, and systematic post-mining land-use planning are vital to minimize ecological damage while supporting resource extraction. Moreover, sustainable forest management approaches should embody a broader paradigm shift. Empowering local communities via the implementation of the Forest Rights Act can bolster conservation at grassroots levels, while integrating principles of reconciliation ecology can help align extractive activities with habitat preservation. Infrastructure planning should incorporate wildlife corridors and measures to reduce habitat fragmentation, and independent audits of afforestation and corporate social responsibility (CSR) initiatives are essential for accountability. Although our classification achieved a high overall accuracy (~90%), future assessments would benefit from finer-resolution data and explicit metrics of fragmentation to enhance understanding of forest dynamics. Nonetheless, this study provides compelling evidence of substantial forest degradation in Keonjhar and Sundargarh, primarily driven by mining-related activities. Without transformative governance frameworks emphasizing ecological accountability and sustainable development, the persistence of these forests and their invaluable ecosystem services remains increasingly at risk.

Acknowledgments

Authors are grateful to Department of Science and Technology (DST), Govt. of India and Vidyasagar University to carry out this study.

Authors' Contributions

Tanushree Basu Roy: Conceptualization, Methodology, Analysis, Visualization, Writing – original draft.

Dipanwita Dutta: Supervision, Project administration, Conceptualization, Methodology, Formal analysis, Visualization, Investigation, Writing – review & editing.

Funding

This research study was financially supported by the Department of Science and Technology (DST), Govt. of Indiato the first author.

Availability of data and materials

The datasets used and/or analyzed during the current study are available from the corresponding author on reasonable request.

Competing interests

The authors declare that they have no competing interests regarding the publication of this paper.

Author details

Department of Remote Sensing and GIS, Vidyasagar University, Midnapore, West Bengal, India.

References

Abdollahnejad, A., Panagiotidis, D., & Surový, P., 2017, Forest canopy density assessment using different approaches – Review 2017: 107–116. https://doi.org/10.17221/110/2016-JFS

Basu, A., & Nayak, N.C., 2011, Underlying causes of forest cover change in Odisha, India. Forest Policy and Economics 13: 563–569. https://doi.org/10.1016/J.FORPOL.2011.07.004

Bhandari, S.K., & Nandy, S., 2024, Forest Aboveground Biomass Prediction by Integrating Terrestrial Laser Scanning Data, Landsat 8 OLI-Derived Forest Canopy Density and Spectral Indices. Journal of the Indian Society of Remote Sensing 52: 813–824. https://doi.org/10.1007/S12524-023-01687-Z/FIGURES/7

Boutsoukis, C., Manakos, I., Heurich, M., & Delopoulos, A., 2019, Canopy Height Estimation from Single Multispectral 2D Airborne Imagery Using Texture Analysis and Machine Learning in Structurally Rich Temperate Forests. Remote Sensing 11, 2853. https://doi.org/10.3390/RS11232853

Bragagnolo, L., da Silva, R.V., & Grzybowski, J.M.V., 2021, Amazon forest cover change mapping based on semantic segmentation by U-Nets. Ecological Informatics 62, 101279. https://doi.org/10.1016/j.ecoinf.2021.101279

Chandrashekhar, B., Saran, S., Raju, P.L.N., & Roy, P.S., 2005, Forest Canopy Density Stratification : How Relevant is Biophysical Spectral Response Modelling Approach ? Geocarto International 20(1): 15–21.

Cohen, W.B., Healey, S.P., Yang, Z., Stehman, S.V., Brewer, C.K., Brooks, E.B., Gorelick, N., Huang, C., Hughes, M.J., Kennedy, R.E., Loveland, T.R., Moisen, G.G., Schroeder, T.A., Vogelmann, J.E., Woodcock, C.E., Yang, L., & Zhu, Z., 2017, How Similar Are Forest Disturbance Maps Derived from Different Landsat Time Series Algorithms? Forests 8: 1–19. https://doi.org/10.3390/f8040098

Crouzeilles, R., Maurenza, D., Prieto, P.V., Barros, F.S.M., Jakovac, C., Ferreira, M.S., Chazdon, R.L., Lindenmayer, D.B., Brancalion, P.H.S., Ceccon, E., Adams, C., Lazos-Chavero, E., Monteiro, L., Junqueira, A.B., Strassburg, B.B.N., & Guariguata, M.R., 2021, Associations between socio-environmental factors and landscape-scale biodiversity recovery in naturally regenerating tropical and subtropical forests. Conservation Letters 14(2). https://doi.org/10.1111/conl.12768

De Pauw, K., Sanczuk, P., Meeussen, C., Depauw, L., De Lombaerde, E., Govaert, S., Vanneste, T., Brunet, J., Cousins, S.A.O., Gasperini, C., Hedwall, P.O., Iacopetti, G., Lenoir, J., Plue, J., Selvi, F., Spicher, F., Uria-Diez, J., Verheyen, K., Vangansbeke, P., & De Frenne, P., 2022, Forest understorey communities respond strongly to light in interaction with forest structure, but not to microclimate warming. New Phytologist 233: 219–235. https://doi.org/10.1111/NPH.17803;WGROUP:STRING:PUBLICATION

Deka, J., & Tripathi, O.P., 2013, Implementation of Forest Canopy Density Model to Monitor Tropical Deforestation 41: 469–475. https://doi.org/10.1007/s12524-012-0224-5

Eckert, S., Hüsler, F., Liniger, H., & Hodel, E., 2015, Trend analysis of MODIS NDVI time series for detecting land degradation and regeneration in Mongolia. Journal of Arid Environments 113: 16–28. https://doi.org/10.1016/j.jaridenv.2014.09.001

Erdody, T.L., & Moskal, L.M., 2010. Fusion of LiDAR and imagery for estimating forest canopy fuels. Remote Sensing of Environment 114: 725–737. https://doi.org/10.1016/J.RSE.2009.11.002

Estoque, R.C., Johnson, B.A., Gao, Y., Dasgupta, R., Ooba, M., Togawa, T., Hijioka, Y., Murayama, Y., Gavina, L.D., Lasco, R.D., & Nakamura, S., 2021, Remotely sensed tree canopy cover-based indicators for monitoring global sustainability and environmental initiatives. Research in Astronomy and Astrophysics 21. https://doi.org/10.1088/1674-4527/21/2/37

Ewers, R.M., & Banks-Leite, C., 2013, Fragmentation Impairs the Microclimate Buffering Effect of Tropical Forests. PLOS ONE 8, e58093. https://doi.org/10.1371/JOURNAL.PONE.0058093

Fasil, M., Surendran, U.P., Gopinath, G., Karimbanakkuzhi, A., & Sahadevan, A.S., 2022, Integration of GIS, remote sensing, and spectral indices for evaluation of forest canopy density model in drought and wet years in Western Ghats region of humid tropical Kerala, India. Arabian Journal of Geosciences 15. https://doi.org/10.1007/s12517-022-10368-z

Food and Agriculture Organisation (FAO), 2010, Global Forest Resources Assessment 2010 - Main report. FAO Forestry Paper 163, 350 pp.

Forkel, M., Carvalhais, N., Verbesselt, J., Mahecha, M.D., Neigh, C.S.R., & Reichstein, M., 2013, Trend Change Detection in NDVI Time Series: Effects of Inter-Annual Variability and Methodology. Remote Sensing 5: 2113–2144. https://doi.org/10.3390/RS5052113

Gao, Si, Zhong, R., Yan, K., Ma, X., Chen, X., Pu, J., Gao, Sicong, Qi, J., Yin, G., & Myneni, R.B., 2023, Evaluating the saturation effect of vegetation indices in forests using 3D radiative transfer simulations and satellite observations. Remote Sensing of Environment 295, 113665. https://doi.org/10.1016/J.RSE.2023.113665

Gillespie, T.W., Ostermann-Kelm, S., Dong, C., Willis, K.S., Okin, G.S., & MacDonald, G.M., 2018. Monitoring changes of NDVI in protected areas of southern California. Ecological Indicators 88: 485–494. https://doi.org/10.1016/j.ecolind.2018.01.031

Godinho, S., Gil, A., Guiomar, N., Neves, N., & Pinto-Correia, T., 2016, A remote sensing-based approach to estimating montado canopy density using the FCD model: a contribution to identifying HNV farmlands in southern Portugal. Agroforestry Systems 90: 23–34. https://doi.org/10.1007/s10457-014-9769-3

Grecchi, R.C., Beuchle, R., Shimabukuro, Y.E., Aragão, L.E.O.C., Arai, E., Simonetti, D., & Achard, F., 2017, An integrated remote sensing and GIS approach for monitoring areas affected by selective logging: A case study in northern Mato Grosso, Brazilian Amazon. International journal of applied earth observation and geoinformation : ITC journal 61: 70–80. https://doi.org/10.1016/j.jag.2017.05.001

Gupta, A., Sharma, S.K., Mishra, A., Singh, G.P., & Singh, C.P., 2024, Effect of mine-derived pollution on photosynthetic pigments of plants in Rajasthan. Vegetos 37: 1833–1842. https://doi.org/10.1007/S42535-024-00992-3/FIGURES/5

Gyawali, A., Adhikari, H., Aalto, M., & Ranta, T., 2024, From simple linear regression to machine learning methods: Canopy cover modelling of a young forest using planet data. Ecological Informatics 82, 102706. https://doi.org/10.1016/J.ECOINF.2024.102706

Hadi, Korhonen, L., Hovi, A., Rönnholm, P., & Rautiainen, M., 2016, International Journal of Applied Earth Observation and Geoinformation The accuracy of large-area forest canopy cover estimation using Landsat in boreal region. International Journal of Applied Earth Observations and Geoinformation 53: 118–127. https://doi.org/10.1016/j.jag.2016.08.009

Hansen, M.C., Wang, L., Song, X.P., Tyukavina, A., Turubanova, S., Potapov, P.V., & Stehman, S.V., 2020, The fate of tropical forest fragments. Science Advances 6. https://doi.org/10.1126/SCIADV.AAX8574/SUPPL_FILE/AAX8574_SM.PDF

Hermes, C., Döpper, A., Schaefer, H.M., & Segelbacher, G., 2016, Effects of forest fragmentation on the morphological and genetic structure of a dispersal-limited, endangered bird species. Nature Conservation 16: 39–58. https://doi.org/10.3897/NATURECONSERVATION.16.10905

Hernández-Clemente, R., Hornero, A., Mottus, M., Penuelas, J., González-Dugo, V., Jiménez, J.C., Suárez, L., Alonso, L., & Zarco-Tejada, P.J., 2019, Early Diagnosis of Vegetation Health From High-Resolution Hyperspectral and

Thermal Imagery: Lessons Learned From Empirical Relationships and Radiative Transfer Modelling. Current Forestry Reports 5: 169–183. https://doi.org/10.1007/s40725-019-00096-1

Himayah, S., Hartono, & Danoedoro, P., 2016, The Utilization of Landsat 8 Multitemporal Imagery and Forest Canopy Density (FCD) Model for Forest Reclamation Priority of Natural Disaster Areas at Kelud Mountain, East Java. IOP Conference Series: Earth and Environmental Science 47. https://doi.org/10.1088/1755-1315/47/1/012043

Hoang, N.T., & Kanemoto, K., 2021, Mapping the deforestation footprint of nations reveals growing threat to tropical forests. Nature Ecology and Evolution 5: 845–853. https://doi.org/10.1038/s41559-021-01417-z

Hota, P., & Behera, B., 2019, Extraction of mineral resources and regional development outcomes: Empirical evidence from Odisha, India. The Extractive Industries and Society 6: 267–278. https://doi.org/10.1016/J.EXIS.2019.03.001

Hota, P., & Behera, B., 2016, Opencast coal mining and sustainable local livelihoods in Odisha, India. Mineral Economics 29: 1–13. https://doi.org/10.1007/S13563-016-0082-7/TABLES/14

Hota, P., & Behera, B., 2015, Coal mining in Odisha: An analysis of impacts on agricultural production and human health. The Extractive Industries and Society 2: 683–693. https://doi.org/10.1016/J.EXIS.2015.08.007

Ismail, M., Hartono, & Danoedoro, P., 2017, The Application of Forest Cover Density (FCD) Model for Structural Composition of Vegetation Changes in Part of Lore Lindu National Park, Central Sulawesi Province. IOP Conference Series: Earth and Environmental Science 98, 012056. https://doi.org/10.1088/1755-1315/98/1/012056

Jamali, S., Jönsson, P., Eklundh, L., Ardö, J., & Seaquist, J., 2015, Detecting changes in vegetation trends using time series segmentation. Remote Sensing of Environment 156: 182–195. https://doi.org/10.1016/J.RSE.2014.09.010

Joshi, C., Leeuw, J. De, Skidmore, A.K., van Duren, I.C., & van Oosten, H., 2006, Remotely sensed estimation of forest canopy density: A comparison of the performance of four methods. International Journal of Applied Earth Observation and Geoinformation 8: 84–95. https://doi.org/10.1016/J.JAG.2005.08.004

Ju, J., & Masek, J.G., 2016, The vegetation greenness trend in Canada and US Alaska from 1984–2012 Landsat data. Remote Sensing of Environment 176: 1–16. https://doi.org/10.1016/J.RSE.2016.01.001

Kganyago, M., Mhangara, P., & Adjorlolo, C., 2021, Estimating Crop Biophysical Parameters Using Machine Learning Algorithms and Sentinel-2 Imagery. Remote Sensing 13, 4314. https://doi.org/10.3390/RS13214314

Kherif, F., & Latypova, A., 2020, Principal component analysis, [in:] Machine Learning: Methods and Applications to Brain Disorders, p. 209–225. https://doi.org/10.1016/B978-0-12-815739-8.00012-2

Korhonen, L., 2011, Estimation of boreal forest canopy cover with ground measurements, statistical models and remote sensing. Dissertationes Forestales 2011. https://doi.org/10.14214/DF.115

Korhonen, L., Ali-sisto, D., & Tokola, T., 2015, Tropical forest canopy cover estimation using satellite imagery and airborne lidar reference data 49.

Korhonen, L., Korhonen, K.T., Rautiainen, M., Stenberg, P., 2006. Estimation of forest canopy cover: A comparison of field measurement techniques. Silva Fennica 40: 577–588.

Korhonen, L., Packalen, P., & Rautiainen, M., 2017, Remote Sensing of Environment Comparison of Sentinel-2 and Landsat 8 in the estimation of boreal forest canopy cover and leaf area index. Remote Sensing of Environment 195: 259–274. https://doi.org/10.1016/j.rse.2017.03.021

Krishna, R.S., Mishra, J., Meher, S., Das, S.K., Mustakim, S.M., & Singh, S.K., 2020, Industrial solid waste management through sustainable green technology: Case study insights from steel and mining industry in Keonjhar, India. Materials Today: Proceedings 33: 5243–5249. https://doi.org/10.1016/J.MATPR.2020.02.949

Kucsicsa, G., Popovici, E.A., Bălteanu, D., Dumitrașcu, M., Grigorescu, I., & Mitrică, B., 2020, Assessing the Potential Future Forest-Cover Change in Romania, Predicted Using a Scenario-Based Modelling. Environmental Modeling and Assessment 25: 471–491. https://doi.org/10.1007/s10666-019-09686-6

Kumar, A., Venkatesh, A.S., Amesh Babu, P.V.R., & Nayak, S., 2012, Genetic Implications of Rare Uraninite and Pyrite in Quartz-Pebble Conglomerates from Sundargarh District of Orissa, Eastern India. Journal of the Geological Society of India 79: 279–286. https://doi.org/10.1007/S12594-012-0040-0

Kumar, J., Talwar, P., & Krishna A.P., 2015, Forest Canopy Density and ASTER DEM based Study for Dense Forest Investigation using Remote Sensing and GIS Techniques around East Singhbhum in Jharkhand, India. International Journal of Advanced Remote Sensing and GIS 4: 1026–1032. https://doi.org/10.23953/cloud.ijarsg.96

Kumar, K., 2014. Confronting Extractive Capital: Social and Environmental Movements in Odisha on JSTOR [WWW Document]. Economic and Political Weekly. URL https://www.jstor.org/stable/24479385 [Accessed 9.9.2025].

Lenk, A., Richter, R., Kretz, L., & Wirth, C., 2024, Effects of canopy gaps on microclimate, soil biological activity and their relationship in a European mixed floodplain forest. Science of The Total Environment 941, 173572. https://doi.org/10.1016/J.SCITOTENV.2024.173572

Lohchab, R.K., & Saini, J.K., 2018, Industrial Pollution Management I: 1–6.

Loi, D.T., Chou, T., & Fang, Y., 2017, Integration of GIS and Remote Sensing for Evaluating Forest Canopy Density Index in Thai Nguyen Province. International Journal of Environmental Science and Development 8(8): 539–542. https://doi.org/10.18178/ijesd.2017.8.8.1012

López García, J., Prado Molina, J., Manzo Delgado, L., & Peralta Higuera, A., 2016, Monitoreo de cambios en la densidad de cobertura forestal en bosque templado usando fotografías aéreas digitales de alta resolución. Investigaciones Geograficas 2016: 59–74. https://doi.org/10.14350/rig.47360

Ma, S., Zhou, Z., Zhang, Y., An, Y., & Yang, G. Bin, 2022, Identification of forest disturbance and estimation of forest age in subtropical mountainous areas based on Landsat time series data. Earth Science Informatics 15: 321–334. https://doi.org/10.1007/s12145-021-00728-w

Magnago, L.F.S., Rocha, M.F., Meyer, L., Martins, S.V., & Meira-Neto, J.A.A., 2015, Microclimatic conditions at forest edges have significant impacts on vegetation structure in large Atlantic forest fragments. Biodiversity and Conservation 24: 2305–2318. https://doi.org/10.1007/s10531-015-0961-1

Martínez, B., & Gilabert, M.A., 2009, Vegetation dynamics from NDVI time series analysis using the wavelet transform. Remote Sensing of Environment 113: 1823–1842. https://doi.org/10.1016/j.rse.2009.04.016

Mengist, W., Soromessa, T., & Feyisa, G.L., 2021, Monitoring Afromontane forest cover loss and the associated socio-ecological drivers in Kaffa biosphere reserve, Ethiopia. Trees, Forests and People 6, 100161. https://doi.org/10.1016/j.tfp.2021.100161

Mishra, B., 2010, Agriculture, Industry and Mining in Orissa in the Post-Liberalisation Era: An Inter-District and Inter-State Panel Analysis on JSTOR [WWW Document]. Economic and Political Weekly. URL https://www.jstor.org/stable/27807027 [Accessed 9.9.2025].

Mishra, M., Santos, C.A.G., Nascimento, T.V.M. do, Dash, M.K., Silva, R.M. da, Kar, D., & Acharyya, T., 2022, Mining impacts on forest cover change in a tropical forest using remote sensing and spatial information from 2001–2019: A case study of Odisha (India). Journal of Environmental Management 302, 114067. https://doi.org/10.1016/J.JENVMAN.2021.114067

Mishra, P.P., & Pujari, A.K., 2008, Impact of mining on agricultural productivity: A case study of the Indian State of Orissa. South Asia Economic Journal 9: 337–350. https://doi.org/10.1177/139156140800900204

Mon, M.S., Mizoue, N., Htun, N.Z., Kajisa, T., & Yoshida, S., 2012, Estimating forest canopy density of tropical mixed deciduous vegetation using Landsat data: a comparison of three classification approaches. International Journal of Remote Sensing 33: 1042–1057. https://doi.org/10.1080/01431161.2010.549851

O'Laughlin, J., Livingston, R.L., Thier, R., Thornton, J.P., Toweill, D.E., & Morelan, L., 1994, Defining and Measuring Forest Health. Journal of Sustainable Forestry 2: 65–85. https://doi.org/10.1300/J091v02n01_03

Pal, S.C., Chakrabortty, R., Malik, S., & Das, B., 2018, Application of forest canopy density model for forest cover mapping using LISS-IV satellite data : a case study of Sali watershed, West Bengal. Modeling Earth Systems and Environment 4: 853-865. https://doi.org/10.1007/s40808-018-0445-x

Palmero-Iniesta, M., Pino, J., Pesquer, L., & Espelta, J.M., 2021, Recent forest area increase in Europe: expanding and regenerating forests differ in their regional patterns, drivers and productivity trends. European Journal of Forest Research 140: 793–805. https://doi.org/10.1007/s10342-021-01366-z

Pei, H., Liu, M., Jia, Y., Zhang, H., Li, Y., & Xiao, Y., 2021, The trend of vegetation greening and its drivers in the Agro-pastoral ecotone of northern China, 2000–2020. Ecological Indicators 129, 108004. https://doi.org/10.1016/j.ecolind.2021.108004

Pfeifer, M., Lefebvre, V., Peres, C.A., Banks-Leite, C., Wearn, O.R., Marsh, C.J., Butchart, S.H.M., Arroyo-Rodríguez, V., Barlow, J., Cerezo, A., Cisneros, L., D'Cruze, N., Faria, D., Hadley, A., Harris, S.M., Klingbeil, B.T., Kormann, U., Lens, L., Medina-Rangel, G.F., Morante-Filho, J.C., Olivier, P., Peters, S.L., Pidgeon, A., Ribeiro, D.B., Scherber, C., Schneider-Maunoury, L., Struebig, M., Urbina-Cardona, N., Watling, J.I., Willig, M.R., Wood, E.M., & Ewers, R.M., 2017, Creation of forest edges has a global impact on forest vertebrates. Nature 551: 187–191. https://doi.org/10.1038/NATURE24457

Plessis, W.P., 1999, Linear regression relationships between NDVI, vegetation and rainfall in Etosha National Park, Namibia. Journal of Arid Environments 42(4): 235–260.

Popradit, A., Srisatit, T., Kiratiprayoon, S., Yoshimura, J., Ishida, A., Shiyomi, M., Murayama, T., Chantaranothai, P., Outtaranakorn, S., & Phromma, I., 2015, Anthropogenic effects on a tropical forest according to the distance from human settlements. Scientific Reports 5, 1–10. https://doi.org/10.1038/srep14689

Prodromou, M., Gitas, I., Themistocleous, K., & Hadjimitsis, D., 2022, The implementation of the Forest Canopy Density (FCD) model for Coniferous ecosystems in Cyprus forests, using Landsat-8 and Sentinel-2 satellite data. https://doi.org/10.5194/EGUSPHERE-EGU22-9865

Radhakrishnan, S., Lakshminarayanan, A.S., Chatterjee, J.M., & Hemanth, D.J., 2020, Forest data visualization and land mapping using support vector machines and decision

trees. Earth Science Informatics 13: 1119–1137. https://doi.org/10.1007/s12145-020-00492-3

Ramsay, M.S., Sgarlata, G.M., Barratt, C.D., Salmona, J., Andriatsitohaina, B., Kiene, F., Manzi, S., Ramilison, M.L., Rakotondravony, R., Chikhi, L., Lehman, S.M., & Radespiel, U., 2023, Effects of Forest Fragmentation on Connectivity and Genetic Diversity in an Endemic and an Invasive Rodent in Northwestern Madagascar. Genes 14, 1451. https://doi.org/10.3390/GENES14071451/S1

Rikimaru, A., & Koganei-shi, K.-C., 2017, Development of forest canopy density mapping and monitoring model using indices of vegetation, bare soil and shadow 1–7.

Rikimaru, A., & Miyatake, S., 2009, Development of forest canopy density mapping and monitoring model using indices of vegetation, bare soil and shadow. Geospatial World 09/01/2009, p. 1–5.

Rikimaru, A., Roy, P.S., & Miyatake, S., 2002, Tropical forest cover density mapping. Tropical Ecology 43: 39–47.

Rodrigues, P., Dorresteijn, I., Guilherme, J.L., Hanspach, J., De Beenhouwer, M., Hylander, K., Bekele, B., Senbeta, F., Fischer, J., & Nimmo, D., 2021, Predicting the impacts of human population growth on forest mammals in the highlands of southwestern Ethiopia. Biological Conservation 256. https://doi.org/10.1016/j.biocon.2021.109046

Sahana, M., Sajjad, H., & Ahmed, R., 2015, Assessing spatio-temporal health of forest cover using forest canopy density model and forest fragmentation approach in Sundarban reserve forest, India. Modeling Earth Systems and Environment 1: 1–10. https://doi.org/10.1007/S40808-015-0043-0/TABLES/2

Santos, C.A.G., do Nascimento, T.V.M., & da Silva, R.M., 2020, Analysis of forest cover changes and trends in the Brazilian semiarid region between 2000 and 2018. Environmental Earth Sciences 79: 1–20. https://doi.org/10.1007/s12665-020-09158-1

Seidler, R., & Bawa, K.S., 2001, Logged forests,.[in:] Levin S.A. (ed.) Encyclopedia of biodiversity. New York: Elsevier, p. 747–760. DOI 10.1016/B0-12-226865-2/00178-4.

Sharma, I., Tongkumchum, P., & Ueranantasun, A., 2021, Regression Analysis of Normalized Difference Vegetation Index (NDVI) to Compare Seasonal Patterns and 15 Year Trend of Vegetation from East to West of Nepal. Nature Environment and Pollution Technology 20: 267–273. https://doi.org/10.46488/NEPT.2021.V20I01.029

Sharma, P., Thapa, R.B., & Matin, M.A., 2020, Examining forest cover change and deforestation drivers in Taunggyi District, Shan State, Myanmar. Environment, Development and Sustainability 22: 5521–5538. https://doi.org/10.1007/s10668-019-00436-y

Singh, S., 2021, Forestry Research in Mine Reclamation in India: Past, Present and Future. Indian Journal of Forestry 43: 10–18. https://doi.org/10.54207/BSMPS1000-2021-82P483

Stojanova, D., Panov, P., Gjorgjioski, V., Kobler, A., & Džeroski, S., 2010, Estimating vegetation height and canopy cover from remotely sensed data with machine learning. Ecological Informatics 5: 256–266. https://doi.org/10.1016/J.ECOINF.2010.03.004

Sudhakar Reddy, C., Saranya, K.R.L., Vazeed Pasha, S., Satish, K.V., Jha, C.S., Diwakar, P.G., Dadhwal, V.K., Rao, P.V.N., & Krishna Murthy, Y.V.N., 2018. Assessment and monitoring of deforestation and forest fragmentation in South Asia since the 1930s. Global and Planetary Change 161: 132–148. https://doi.org/10.1016/j.gloplacha.2017.10.007

Syakur, S., Kausar, A.N., & Fazlina, Y.D., 2025' Analysis of mangrove vegetation distribution and density in East Aceh Regency. IOP Conference Series: Earth and Environmental Science 1477, 012011. https://doi.org/10.1088/1755-1315/1477/1/012011

Tian, F., Fensholt, R., Verbesselt, J., Grogan, K., Horion, S., & Wang, Y., 2015, Evaluating temporal consistency of long-term global NDVI datasets for trend analysis. Remote Sensing of Environment 163: 326–340. https://doi.org/10.1016/j.rse.2015.03.031

Tian, Z., Fan, J., Yu, T., de Leon, N., Kaeppler, S.M., & Zhang, Z., 2025, Mitigating NDVI saturation in imagery of dense and healthy vegetation. ISPRS Journal of Photogrammetry and Remote Sensing 227: 234–250. https://doi.org/10.1016/J.ISPRSJPRS.2025.06.013

Vancutsem, C., Achard, F., Pekel, J.F., Vieilledent, G., Carboni, S., Simonetti, D., Gallego, J., Aragão, L.E.O.C., & Nasi, R., 2021, Long-term (1990–2019) monitoring of forest cover changes in the humid tropics. Science Advances 7: 1–22. https://doi.org/10.1126/sciadv.abe1603

Verrelst, J., Malenovský, Z., Van der Tol, C., Camps-Valls, G., Gastellu-Etchegorry, J.P., Lewis, P., North, P., & Moreno, J., 2019, Quantifying Vegetation Biophysical Variables from Imaging Spectroscopy Data: A Review on Retrieval Methods. Surveys in Geophysics 40: 589–629. https://doi.org/10.1007/s10712-018-9478-y

Wang, C., Feng, M.C., Yang, W. De, Ding, G.W., Sun, H., Liang, Z.Y., Xie, Y.K., & Qiao, X.X., 2016, Impact of spectral saturation on leaf area index and aboveground biomass estimation of winter wheat. Spectroscopy Letters 49: 241–248. https://doi.org/10.1080/00387010.2015.1133652; WGROUP:STRING:PUBLICATION

Wang, X., Shi, J., Wang, C., Gao, C., & Zhang, F., 2023, Remote Sensing Inversion and Mapping of Typical Forest Stand Age in the Loess Plateau. Remote Sensing 15, 5581. https://doi.org/10.3390/RS15235581

Xiong, Y., & Wang, H., 2022, Spatial relationships between NDVI and topographic factors at multiple scales in a watershed of the Minjiang River, China. Ecological

Informatics 69, 101617. https://doi.org/10.1016/j.ecoinf.2022.101617

Xue, J., & Su, B., 2017, Significant remote sensing vegetation indices: A review of developments and applications. Journal of Sensors 2017. https://doi.org/10.1155/2017/1353691

Yang, Y., Tian, Q., & Xu, L., 2007, A new approach for estimating the vegetation fraction in mountainous area. https://doi.org/10.1117/12.760492 6752: 530–538. https://doi.org/10.1117/12.760492

Zhang, Z., Jin, W., Dou, R., Cai, Z., Wei, H., Wu, T., Yang, S., Tan, M., Li, Z., Wang, C., Yin, G., & Xu, B., 2023, Improved Estimation of Leaf Area Index by Reducing Leaf Chlorophyll Content and Saturation Effects Based on Red-Edge Bands. IEEE Transactions on Geoscience and Remote Sensing 61. https://doi.org/10.1109/TGRS.2023.3270712

Zoungrana, B.J.B., Conrad, C., Thiel, M., Amekudzi, L.K., & Da, E.D., 2018, MODIS NDVI trends and fractional land cover change for improved assessments of vegetation degradation in Burkina Faso, West Africa. Journal of Arid Environments 153: 66–75. https://doi.org/10.1016/j.jaridenv.2018.01.005